JOURNAL OF MATERIALS & CONSTRUCTION
Journal of Materials and Construction
ISSN 2734-9438
Website: www. jomc.vn

An investigation of seepage flow through homogenous embankment dams using an iteration technique for determining the free surfaces

Thi Tuyet Giang Vo[1,2] and Vo Trong Nguyen[1,2*]

[1] Faculty of Civil Engineering, Ho Chi Minh City University of Technology (HCMUT), 268 Ly Thuong Kiet Street, District 10, Ho Chi Minh City, Vietnam

[2] Vietnam National University Ho Chi Minh City, Linh Trung Ward, Thu Duc District, Ho Chi Minh City, Vietnam

KEYWORDS

embankment, finite element method, free surface, seepage, un-saturated flow

ABSTRACT

This paper presents the application of the finite element method into solving the balance equation of seepage flows within the porous media. More specifically, these seepage flows occur within homogenous embankment dams. With the specific boundary conditions of water levels in the upstream and downstream sides, the seepage mechanism takes place, generating the unsaturated zones and the saturated ones as well. The demarcation surfaces between the un-saturated and saturated zones are called the free surfaces. For determining these free surfaces, an algorithm of loop is employed, and the convergence is required to locate the free surfaces. This paper combines the relevant ideas into a program using the Python programming language. Next, a case is shown using the current sub-routine considering the convergence of the solution and comparing it to the outcome of a popular software of seepage analysis SEEP/W. The results show that the algorithm used for locating the free surface is acceptable when dealing with this type of seepage mechanism.

1. Introduction

In the area of hydraulic structures, since the relevant works interact with water, seepage usually occurs, and this topic always plays an important role in the field. **Error! Reference source not found.** shows the two common types of seepage through the works.

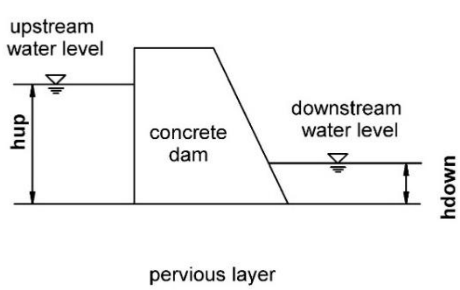

(a)

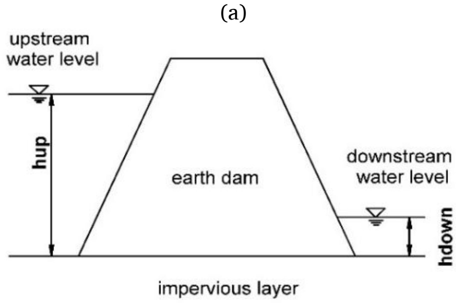

(b)

Figure 1. Two common types of seepage through dams, (a) through concrete dams and (b) through embankment dams.

In **Error! Reference source not found.**a, the seepage mechanism is simpler as the seepage zone is fully saturated. However, the one in **Error! Reference source not found.**b is more complicated since within the seepage zone, there are the un-saturated as well as saturated portions. The interface between two portions has the pore-water pressure equal to zero. This interface is called the free surface and is not prior known, so we need an algorithm to determine it.

Due to the rapid development of computer science and engineering, numerical methods such as finite difference methods, boundary element methods, finite element methods have been used for solving this problem, replacing the analytical methods that contain the simplifications. In the early stage, when the un-saturated soil mechanics were still limited, one assumed the free surfaces as the boundary of the saturated and fully dried zones above. The studies following this approach can be listed as Neuman and Witherspoon [1], Desai [2], Bathe and Khoshgoftaar [3], Lacy and Prevost [4], Cividini and Gioda [5], Leontiev and Huacasi [6], Bardet and Tobita [7]. These studies made a big contribution at the time but not considering the unsaturation to some extent leads to inappropriate outcomes.

When the un-saturated soil theory had a significant development, the application of the un-saturated soils into the analysis of soil mechanics and seepage flows has become more widespread [8]. The studies relating to this trend can be listed as follows: Neuman [9], Desai and Li [10], Papagianakis and Fredlund [11]. The use of the un-saturated soil theory has brought about more appropriate results since the fundamentals of seepage have been thoroughly examined. However, this combination leads to the complication of analysis as to the high

*Corresponding author: nguyenvotrong@hcmut.edu.vn

Received 26/10/2024, Revised 8/11/2024, Accepted 11/11/2024
Link DOI: https://doi.org/10.54772/jomc.v14i02.815

non-linearity.

Currently, the determination of free surfaces has gained significant achievement. Commercial software such as SEEP/W can easily solve this problem. However, along with the goal for implementing our own seepage modelling to further investigations of groundwater extraction, uncertainty in soil properties in seepage flows, we have implemented our own program to determine the free surface. In this study, this idea is applied into the seepage mechanism through homogenous embankment dams. The paper demonstrates an example to check the convergence of the algorithm and compares it with outcome using SEEP/W to see the accuracy of our program.

2. The governing equation of seepage mechanism in two-direction analysis

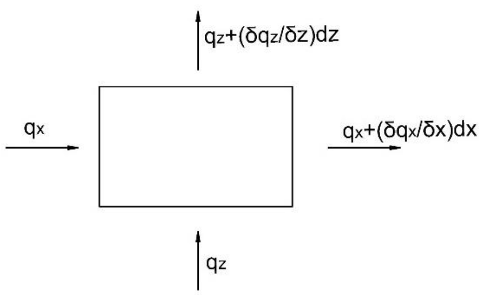

Figure 2. The differential element of seepage mechanism in 2-D analysis.

Using **Error! Reference source not found.**, the balance equation in this case is as follows:

$$Q_{out} - Q_{in} = 0 \quad (1)$$

where, Q_{out} and Q_{in} are the flowrates of the seepage flows entering and leaving the differential element. The components in **Error! Reference source not found.** can be presented as follows (where, K_x and K_z are the hydraulic conductivities in x and z directions; L and T are the dimensions of length and time; the width of the element perpendicular to the elemental plane is one length unit):

$$q_x = -K_x \frac{\partial H}{\partial x} \text{ và } q_z = -K_z \frac{\partial H}{\partial z} \text{ (the dimension of } L^3/T/L^2) \quad (2)$$

$$Q_{out} - Q_{in} = \frac{\partial q_x}{\partial x} dx \times dz \times 1 + \frac{\partial q_z}{\partial z} dx \times dz \times 1 = 0 \quad (3)$$

$$Q_{out} - Q_{in} = \frac{\partial}{\partial x}\left(-K_x \frac{\partial H}{\partial x}\right) dx \times dz \times 1 + \frac{\partial}{\partial z}\left(-K_z \frac{\partial H}{\partial z}\right) dx \times dz \times 1 = 0 \quad (4)$$

Finally, the governing equation describing this seepage mechanism is as follows:

$$\frac{\partial}{\partial x}\left(K_x \frac{\partial H}{\partial x}\right) + \frac{\partial}{\partial z}\left(K_z \frac{\partial H}{\partial z}\right) = 0 \quad (5)$$

where H is the hydraulic head.

3. The Galerkin finite element method

This section is to describe the basic ideas of the Galerkin finite element method which is employed within this study [12]. When constructing the finite element method based on the Galerkin approach, we consider the differential equation (this equation is used for illustrative purposes only):

$$\frac{d^2 y}{dx^2} + f(x) = 0 \quad (x_a \le x \le x_b) \quad (6)$$

and the boundary conditions (**Error! Reference source not found.**):

$$y(x_a) = y_a \text{ and } y(x_b) = y_b \quad (7)$$

An approximate solution is assumed in the form

$$y^*(x) = \sum_{i=1}^{M+1} y_i n_i(x) \quad (8)$$

where y_i is the value of the solution function at $x = x_i$ and $n_i(x)$ is a corresponding trial function.

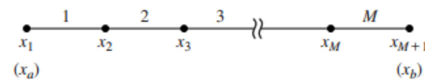

Figure 3. Domain x_a ≤ x ≤ x_b discretized into M elements.

Substitution of the assumed solution (8) into the governing equation (6) yields the residual:

$$R(x; y_i) = \sum_{i=1}^{M+1} \left[\frac{d^2 y^*}{dx^2} + f(x)\right] = \sum_{i=1}^{M+1} \left[\frac{d^2}{dx^2}[y_i n_i(x)] + f(x)\right] \quad (9)$$

to which the application of Galerkin's weighted residual method is used, using each trial function as a weighting function, to obtain:

$$\int_{x_a}^{x_b} n_j(x) R(x; y_i) dx = \int_{x_a}^{x_b} n_j(x) \sum_{i=1}^{M+1} \left[\frac{d^2}{dx^2}[y_i n_i(x)] + f(x)\right] dx \quad (j = 1, M + 1) \quad (10)$$

and this equation can be expressed as:

$$\int_{x_j}^{x_{j+1}} n_j(x) \left[\frac{d^2}{dx^2}[y_j n_j(x) + y_{j+1} n_{j+1}(x)] + f(x)\right] dx = 0 \quad (j = 1, M + 1) \quad (11)$$

Integration of Equation (11) yields $M + 1$ algebraic equations in the $M + 1$ unknown nodal solution values y_j, and these equations can be written in the matrix form

$$[K_{FE}]\{y\} = \{F\} \quad (12)$$

where, $[K_{FE}]$ is the system stiffness matrix, $\{y\}$ is the vector of nodal displacements and $\{F\}$ is the vector of nodal forces. Terms such as stiffness, displacement and force are used in structural mechanics but in this study these terms become hydraulic conductivity, hydraulic head and flux rate instead. Equation (10) is the formal statement of the Galerkin finite element method and includes both element formation and system assembly steps.

4. Finite element formulation

In developing a finite element approach to two-dimensional seepage, we assume a two-dimensional element having M nodes such that the hydraulic-head distribution in the element is described by:

$$H(x, z) = \sum_{i=1}^{M} N_i(x, z) H_i = [N]\{H\} \quad (13)$$

where, $N_i(x, z)$ is the interpolation function associated with nodal hydraulic head H_i, $[N]$ is the row matrix of interpolation functions, and $\{H\}$ is the column matrix (vector) of nodal hydraulic head. Applying Galerkin's finite element method, the residual equations corresponding to Equation (5) are:

$$\iint_A N_i(x,z)\left[\frac{\partial}{\partial x}\left(tK_x\frac{\partial H}{\partial x}\right)+\frac{\partial}{\partial z}\left(tK_z\frac{\partial H}{\partial z}\right)\right]\mathrm{d}A = 0 \quad (i=1,M) \tag{14}$$

where, the thickness t is assumed constant and the integration is over the area of the element (for 2-D analysis, the thickness t is usually taken as one length unit such as one meter). The mathematical manipulation and using the Green-Gauss theorem in the plane leads to:

$$t\iint_A \left[\frac{\partial}{\partial x}\left(K_x\frac{\partial H}{\partial x}\right)N_i+\frac{\partial}{\partial z}\left(K_z\frac{\partial H}{\partial z}\right)N_i\right]\mathrm{d}A = -\mathrm{t}\oint_S (q_x n_x + q_z n_z)N_i dS - t\iint_A \left[K_x\frac{\partial H}{\partial x}\frac{\partial N_i}{\partial x} + K_z\frac{\partial H}{\partial z}\frac{\partial N_i}{\partial z}\right]\mathrm{d}A \tag{15}$$

where, n_x and n_z are the x and z components of the outward unit vectors normal (perpendicular) to the periphery.

Returning to the Galerkin residual equation represented by Equation (14) and substituting the relations developed via the Green-Gauss theorem, Equation (14) becomes:

$$\iint_A \left[K_x\frac{\partial H}{\partial x}\frac{\partial N_i}{\partial x}+K_z\frac{\partial H}{\partial z}\frac{\partial N_i}{\partial z}\right]\mathrm{td}A = -\mathrm{t}\oint_S (q_x n_x + q_z n_z)N_i dS \quad (i=1,M) \tag{16}$$

as the system of M equations for the two-dimensional finite element formulation via Galerkin's method. At this point, we convert to matrix notation for ease of illustration by employing Equation (13) to convert Equation (16) to:

$$\iint_A \left[K_x\left[\frac{\partial N}{\partial x}\right]^T\left[\frac{\partial N}{\partial x}\right]+K_z\left[\frac{\partial N}{\partial z}\right]^T\left[\frac{\partial N}{\partial z}\right]\right]\{H^{(e)}\}\mathrm{td}A = -\oint_S q_s n_s [N]^T t dS \tag{17}$$

which is of the form

$$\left[K_{FE}^{(e)}\right]\{H^{(e)}\} = \left\{F_q^{(e)}\right\} \tag{18}$$

where $\left[K_{FE}^{(e)}\right]$ is the element hydraulic conductivity matrix (the subscript e is used for differentiating from the global matrix); $\left\{F_q^{(e)}\right\}$ is the element nodal flux rate vector. Assuming the environment is isotropic so $K_x = K_z = K$:

$$\left[K_{FE}^{(e)}\right] = K\iint_A \left[\left[\frac{\partial N}{\partial x}\right]^T\left[\frac{\partial N}{\partial x}\right]+\left[\frac{\partial N}{\partial z}\right]^T\left[\frac{\partial N}{\partial z}\right]\right]\mathrm{td}A \tag{19}$$

which for an element having M nodes is an M×M symmetric matrix. And the element nodal flux vector is:

$$\left\{F_q^{(e)}\right\} = -\oint_S q_s n_s [N]^T t dS = -\oint_S q_s n_s \{N\} t dS \tag{20}$$

5. Boundary conditions

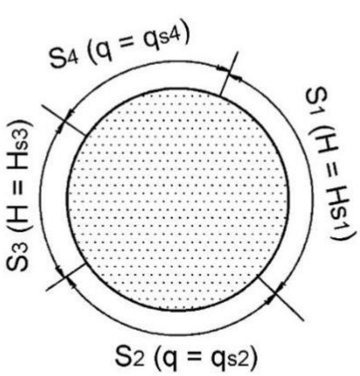

Figure 4. Types of boundary conditions for two-dimensional seepage analysis.

This analysis normally consists of two types. **Error! Reference source not found.** shows the example: in portion S_1, the hydraulic head H is prescribed as H_{s1}. In modelling, all the nodes located in this portion have known hydraulic heads and the values that need to be found are the nodal flux rates (the dimension is $\frac{L^3}{TL} = \frac{L^2}{T}$ as to the plane analysis). This boundary type is called H-type. The portion S_2 has the known flux values q as q_{s2} (since these values are distributed in a length unit of this portion so the dimension is $\frac{L^3}{TLL} = \frac{L}{T}$). This boundary type is called Q-type. Therefore, all the nodes located within this portion have the rates calculated using (20). The similarity is applied to portions S_3 and S_4. In this analysis, since all the Q-type boundaries have the flux distribution $q_s = 0$ so at the beginning all the flux values by default equal to zero. However, due to the free-surface determination, some boudaries need to be uniquely examined and described in the coming section.

6. Element matrix formulation

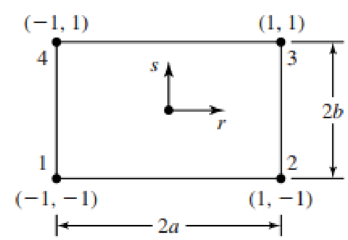

Figure 5. A rectangular element of width 2a and height 2b.

Using the normalized coordinates r and s (**Error! Reference source not found.**), the interpolation functions for four-node rectangular element are:

$$\begin{aligned} N_1(r,s) &= \frac{1}{4}(1-r)(1-s)\\ N_2(r,s) &= \frac{1}{4}(1+r)(1-s)\\ N_3(r,s) &= \frac{1}{4}(1+r)(1+s)\\ N_4(r,s) &= \frac{1}{4}(1-r)(1+s) \end{aligned} \tag{21}$$

The finite element techniques are employed, leading to the element stiffness matrix as follows:

$$\left[K_{FE}^{(e)}\right] = \begin{bmatrix} K_{11}^{(e)} & K_{12}^{(e)} & K_{13}^{(e)} & K_{14}^{(e)} \\ K_{21}^{(e)} & K_{22}^{(e)} & K_{23}^{(e)} & K_{24}^{(e)} \\ K_{31}^{(e)} & K_{32}^{(e)} & K_{33}^{(e)} & K_{34}^{(e)} \\ K_{41}^{(e)} & K_{42}^{(e)} & K_{43}^{(e)} & K_{44}^{(e)} \end{bmatrix} \tag{22}$$

The following is an example of calculating one component within the matrix $\left[K_{FE}^{(e)}\right]$:

$$K_{11}^{(e)} = Ktab\int_{-1}^{1}\int_{-1}^{1}\left[\frac{(s-1)^2}{16}\frac{1}{a^2}+\frac{(r-1)^2}{16}\frac{1}{b^2}\right]dr\,ds \tag{23}$$

where, K is the hydraulic conductivity; t is the element thickness; 2a and 2b are the width and height of the element in the natural coordinates (r, s) (**Error! Reference source not found.**). The other components are similarly calculated. However, the integral of Equation

(23) is performed using numerical integral of Gaussian integration at the points $r_i, s_j = \pm 0.57735$ with the weighting factors $W_i, W_j = 1.0$ and $i, j = 1.2$. Therefore, we have:

$$K_{11}^{(e)} = Kt\frac{b}{a}\sum_{i=1}^{2}\sum_{j=1}^{2}\frac{1}{16}W_iW_j\left(s_j-1\right)^2 + Kt\frac{a}{b}\sum_{i=1}^{2}\sum_{j=1}^{2}\frac{1}{16}W_iW_j(r_i-1)^2 \quad (24)$$

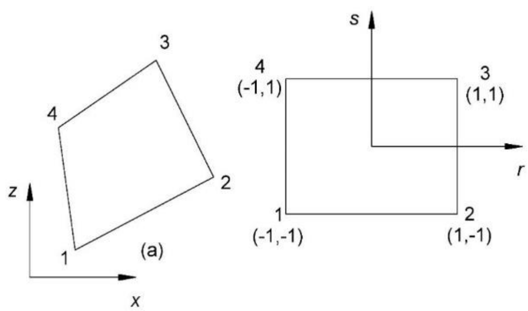

Figure 6. (a) A four-node, two-dimensional iso-parametric element; (b) The parent element in natural coordinates.

The meshes automatically generated usually are not rectangular shapes but quadrilateral shapes (**Error! Reference source not found.**). Then, the existing theory suggests using the iso-parametric formulation as follows:

$$K_{11}^{(e)} = Kt\frac{b}{a}\sum_{i=1}^{2}\sum_{j=1}^{2}\frac{1}{16}W_iW_j\left(s_j-1\right)^2\left|J\left(r_i,s_j\right)\right| + Kt\frac{a}{b}\sum_{i=1}^{2}\sum_{j=1}^{2}\frac{1}{16}W_iW_j(r_i-1)^2\left|J\left(r_i,s_j\right)\right| \quad (25)$$

where, $\left|J\left(r_i,s_j\right)\right|$ is the determinant of Jacobi matrix at coordinates r_i and s_j as follows:

$$[J] = \begin{bmatrix} J_{11} & J_{12} \\ J_{21} & J_{22} \end{bmatrix} = \begin{bmatrix} \frac{\partial x}{\partial r} & \frac{\partial z}{\partial r} \\ \frac{\partial x}{\partial s} & \frac{\partial z}{\partial s} \end{bmatrix} \quad (26)$$

The following is an example of calculating one component of the Jacobi matrix:

$$J_{11} = \frac{\partial x}{\partial r} = \sum_{1}^{4}\frac{\partial N_i}{\partial r}x_i = \frac{1}{4}[(s-1)x_1 + (1-s)x_2 + (1+s)x_3 - (1+s)x_4] \quad (27)$$

Combining all the element matrices leads to the global equation as follows:

$$[K_{FE}]\{H\} = \{F_q\} \quad (28)$$

where, $[K_{FE}]$ is the global hydraulic conductivity matrix of the size of $M_T \times M_T$ with M_T as total number of the nodes of the system; $\{H\}$ is the global hydraulic-head vector, the size of $M_T \times 1$; and $\{F_q\}$ is the global nodal flux rates, the size of $M_T \times 1$.

7. Un-saturated hydraulic conductivity and free surface

As presented, the hydraulic conductivity K appears in the equations for calculating the hydraulic conductivity matrices [i.e. Equation (25)]. The seepage flow with the dam body (**Error! Reference source not found.**) generates the un-saturated zone above the saturated one (the free surface is the boundary to separate these two zones). This un-saturated zone still has the seepage flow but the hydraulic conductivities within these zones are adjusted (less than the original saturated ones). This study employs the model of van Genuchten [13] for calculating the un-saturated hydraulic conductivities. Based on this theory, the un-saturated hydraulic conductivities depend on the pressure heads at the interest points (denoted by h) and can be presented as follows:

$$K(h) = K_sK_r(h) \quad (29)$$

where, K_s is the saturated hydraulic conductivity and $K_r(h)$ is the normalized form, h is the pressure head so equal to hydraulic head minus the elevation at the point. The values of $K_r(h)$ can be calculated based on two parameters α and n. The values of $K_r(h)$ equal one if the pressure head h greater than zero (at the saturated state) and vice versa (e.g. at the unsaturated state, pressure head h less than or equal to zero, $K_r(h)$ is less than one). The equation of K_r can be used [13, 14] as follows:

$$K_r = \frac{\left[1-(\alpha P^{n-1})\left(1+(\alpha P^n)\right)^{-m}\right]^2}{[(1+\alpha P)^n]^{m/2}} \quad (30)$$

where P is matrix suction (kPa) (matrix suction is defined as difference between pore air pressure and pore water pressure); α is a parameter (kPa^{-1}); n is a parameter; m is a parameter calculated as $m = 1 - 1/n$ (α and n are the empirical parameters determined from the experiments).

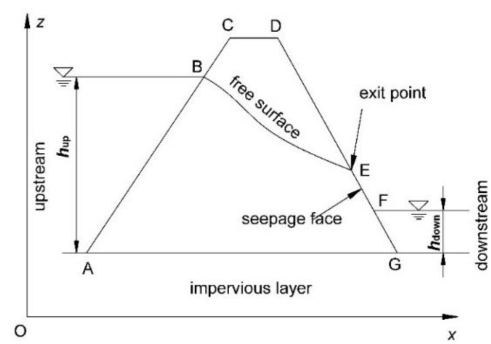

Figure 7. The seepage mechanism within a homogenous embankment dam.

Error! Reference source not found. shows an example of a homogenous embankment dam constructed on an impervious foundation layer. The upstream-side water level is as high as h_{up} compared to the ground level and the downstream-side one h_{down}. The free surface generated within the dam body has the exit point E located higher than the downstream water level. These conditions lead to the following boundary conditions (see **Error! Reference source not found.**):

- The boundaries AB and GF have the H-type boundary of the upstream and downstream hydraulic water levels respectively.
- The boundary BCD is above the saturated zone. Theoretically, there can be the un-saturated flows leaving these boundaries. However, these flow rates are unsignificant compared to the saturated flows and to simplify the numerical solution these boundaries can be treated as non-flow boundaries (or Q-type boundaries and the values of F_q equal to zero). The popular software in seepage analysis of SEEP/W also employs these boundary types when dealing with these types of seepage.

- The boundary DF is more complicated since there is an exit point E appearing within this boundary. The portion EF is called seepage face, and it is expected to have the leaving flows out of the dam body. When dealing with this type of seepage, the user can anticipate which portions contain the exit points and treat these portions based on a unique procedure described in the following section. In popular software SEEP/W, these portions are marked as 'potential seepage face' and the software employs the procedure to determine the exit point and the free surface.

The procedure of determining the exit point or the seepage face within the 'potential seepage face' (DF in the problem in **Error! Reference source not found.**) is presented as follows ([9] and [14]):

- At the beginning, the boundary condition Q-type is set ($F_q = 0$ at all the nodes within this boundary DF). The problem is solved using Equation (28) with the given boundary conditions. Therefore, the free surface and exit point or seepage face are determined. The free surface is determined through the pore water pressure field and using the interpolation technique to get the points of pore water pressure of zero.
- Within the seepage face, if the pressure heads are greater than zero (i.e. the hydraulic heads H are greater than their elevations) it is unacceptable. This is, the Q-type ($F_q = 0$) for this boundary is incorrect so that the procedure converts the such nodes' boudaries to the H-type with pressure heads h of zero (the hydraulic heads H equal the nodes' elevations).
- Based on the outcomes of the next step, if there are the nodes of pressure heads are zero but the flux rates at these nodes are greater than zero (i.e. there are the flows entering the dam body) it is also unacceptable. These kinds of nodes are converted to Q-type ($F_q = 0$).
- The procedure is continued until all the nodes within the seepage face have the pressure heads equal to zero and the flux rates less and equal to zero.

8. Flowchart

This section presents the flowchart for programming the program combining all the above-mentioned ideas. The programming language used in this study is Python. As mentioned, this problem has two aspects needing to be solved using the iteration technique (the flowchart is presented in **Error! Reference source not found.**):

- The first one relates to adjusting the hydraulic conductivities to adapt to calculated pressure heads at the interest points (h). For example, at the beginning, the Q-type and H-type boundary conditions are set as presented in the previous sections. Equation (28) is solved using the saturated hydraulic conductivity for the entire dam body. The calculated pressure heads at all the Gaussian nodes are used for re-calculating the hydraulic conductivities at these nodes, leading to change the element hydraulic conductivity matrices through the equations [e.g. Equation (25)]. The stopping condition for this loop is based on the difference between two consecutive results of total flow rates through the dam body. And the stopping difference is less than 0,01 %. The loop for changing the hydraulic conductivities due to un-saturation is called US loop (US stands for the un-saturation).
- The second one relates to the change of the free surface and seepage face. This loop is called SF (SF stands for the seepage face).

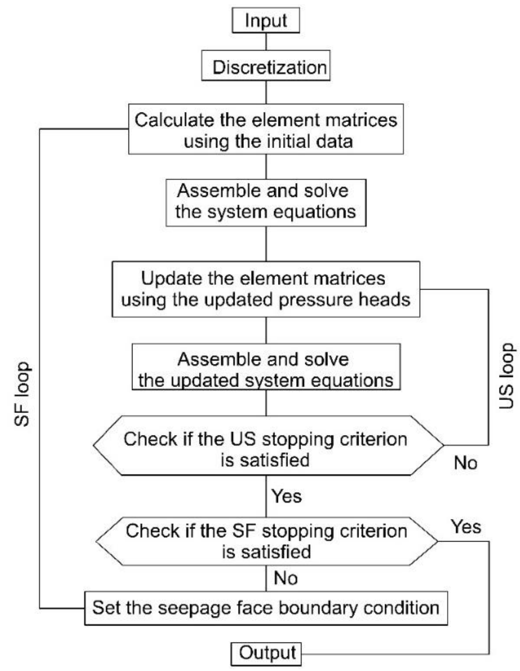

Figure 8. The flowchart of the program.

9. Results and discussion

This study employs a problem presented in **Error! Reference source not found.**. Hence, the simple shape of square embankment dam is considered: the length of a side is 10 m. The heights (compared to the ground level) of the upstream and downstream water levels are $h_{up} = 8$ m and $h_{down} = 2$ m, respectively. The foundation is impervious and the soil used for the modelling has relevant parameters shown in Table 1: K_s is the saturated hydraulic conductivity, the parameters α and n are used for van Genuchten model [13] to calculate the relevant un-saturated hydraulic conductivities.

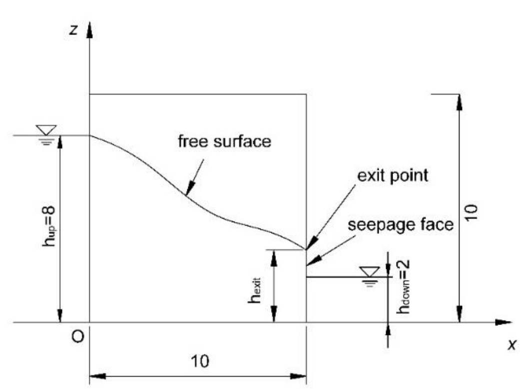

Figure 9. The problem shape used for the investigation of the

algorithm (the length dimension is meter).

Table 1. The soil's parameters.

K_s (m/s)	α (kPa-1)	n
10^{-4}	0.10	2.5

For the discretization, we employ a tool of Gmsh [15]. This tool can create triangular and quadrilateral elements. The mesh sizes are defined by a parameter called size factor. **Error! Reference source not found.** shows the mesh used in this example: the mesh employs quadrilaterals of four Gaussian points and the size factor of 0,3 leading to the interest zone having 1464 nodes and 1393 elements (**Error! Reference source not found.**).

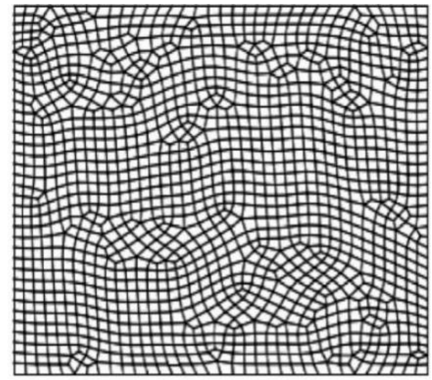

Figure 10. Discretization using quadrilateral elements.

The nodes located within the seepage face (the nodes are governed by the SF loop) are shown in

We employ the simulation using SEEP/W [14]. The same geometry as well as the parameters of van Genuchten model are used in SEEP/W. **Error! Reference source not found.** and **Error! Reference source not found.** show the comparation. The insignificant differences in the heights of the free surfaces and the flowrates through the whole dams demonstrate the encouragement of our own program.

te to the seepage face.

and **Error! Reference source not found.**. In this modeling, the program performs 4 loop steps relating to the seepage face (SF loop). After step 1, the seepage face has 7 nodes that are not satisfied with the stopping criterion as all the pressure heads are greater than zero. Therefore, the boundary condition is changed for the next step. Finally, the stopping criterion is satisfied in step 4.

Besides, the flowchart in **Error! Reference source not found.** shows that in each step of SF, there is a loop relating to changing the un-saturated hydraulic conductivities (US loop). **Error! Reference source not found.** shows the US loops of SF steps 1 and 4. The results show that in SF step 1, the algorithm needs 6 iterations of the US loop and the SF step 4 needs 9 US iterations to achieve the convergence.

We employ the simulation using SEEP/W [14]. The same geometry as well as the parameters of van Genuchten model are used in SEEP/W. **Error! Reference source not found.** and **Error! Reference source not found.** show the comparation. The insignificant differences in the heights of the free surfaces and the flowrates through the whole dams demonstrate the encouragement of our own program.

Table 2. The results relate to the seepage face.

Step	h_{exit} (m)	Nodes	x (m)	z (m)	Q ($\times 10^7$ $m^3/s/m$)	h (m)	Boundary conditions for the next step
1	4,00	46	10	2.29	0	0.60	H-type
		47	10	2.57	0	0.71	H-type
		48	10	2.86	0	0.70	H-type
		49	10	3.14	0	0.63	H-type
		50	10	3.43	0	0.52	H-type
		51	10	3.71	0	0.37	H-type
		52	10	4.00	0	0.19	H-type
2	4,00	46	10	2.29	-3.34	0	H-type
		47	10	2.57	-2.53	0	H-type
		48	10	2.86	-1.94	0	H-type
		49	10	3.14	-1.38	0	H-type
		50	10	3.43	-0.70	0	H-type
		51	10	3.71	2.66	0	Q-type
		52	10	4.00	1.42	0	Q-type

Table 2. The results relate to the seepage face.

Step	h_{exit} (m)	Nodes	x (m)	z (m)	Q ($\times 10^7$ $m^3/s/m$)	h (m)	Boundary conditions for the next step
3	3,43	46	10	2.29	-3.29	0	H-type
		47	10	2.57	-2.46	0	H-type
		48	10	2.86	-1.82	0	H-type
		49	10	3.14	-1.09	0	H-type
		50	10	3.43	+0.20	0	Q-type
4	3,00	46	10	2.29	-3.29	0	(the stopping condition is met)
		47	10	2.57	-2.45	0	(the stopping condition is met)
		48	10	2.86	-1.80	0	(the stopping condition is met)

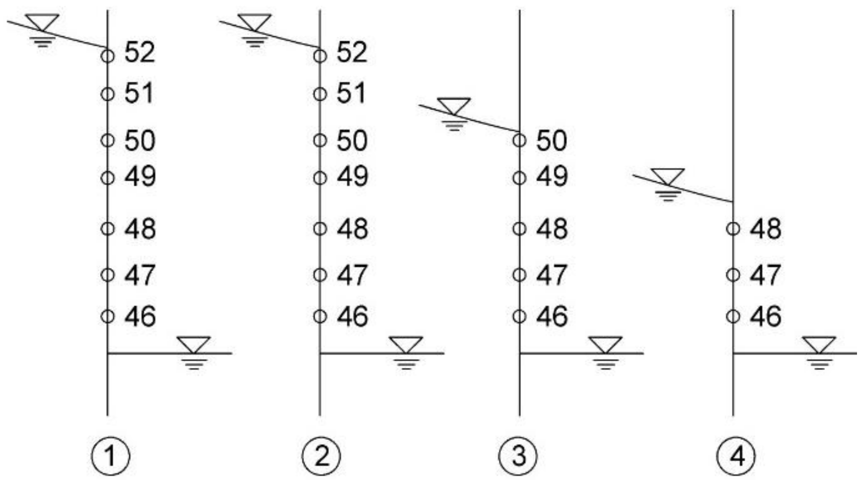

Figure 11. The change of the seepage face through the loop steps.

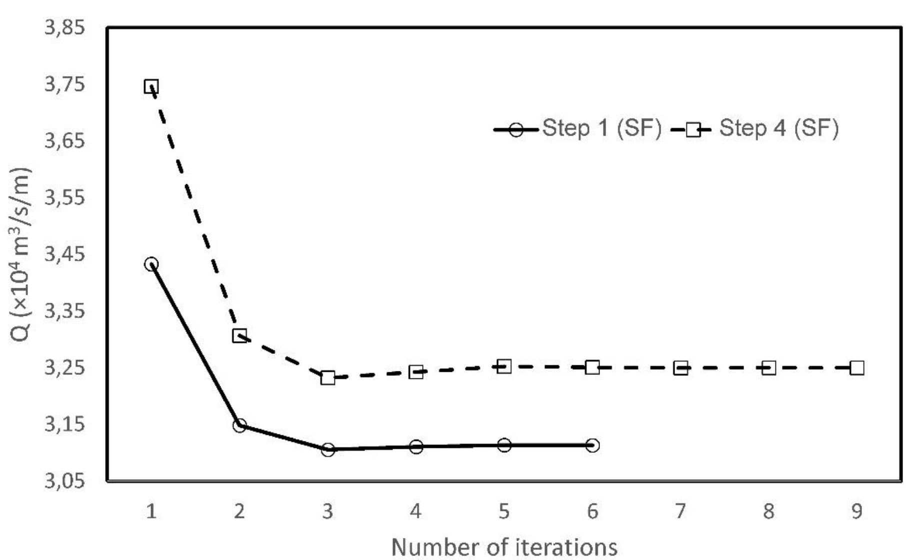

Figure 12. The results of total flow through the dam body relating to the US loop.

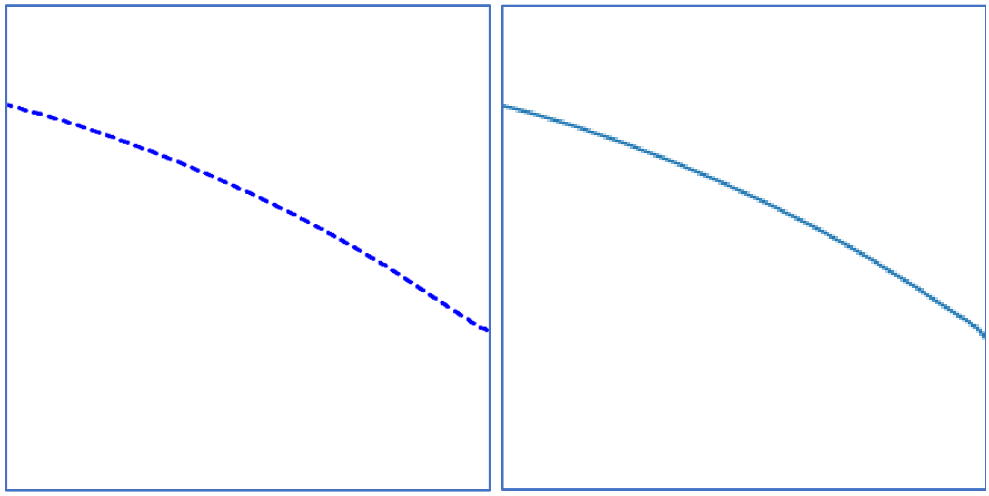

Figure 13. Comparation of the results from SEEP/W and the current model: the left-side curve relates to SEEP/W and the right-side the current model (the vertical axis is z-axis, and the horizontal one is x-axis).

Table 3. Comparison of outcomes from the current model and SEEP/W (h_2 is the height of the free surface compared to the ground elevation at x = 2 m).

Items	SEEP	The current model	Differences (%)
h2 (m)	7.376	7.391	0.19
h5 (m)	6.183	6.187	0.06
h8 (m)	4.572	4.570	0.04
h10 (m) (exit point)	3.344	3.436	2.67
Q ($\times 10^4$ m^3/s/m)	3.2252	3.2246	0.02

9. Conclusion

This study concentrates on an algorithm for determining the free surfaces of the seepage mechanism through homogenous embankment dams. The program employs the existing theories of the Galerkin finite element method, the van Genuchten un-saturated hydraulic conductivity. An algorithm of iteration is used to determine the free surfaces based on the loop for adjusting the hydraulic conductivity due to the un-saturation and the loop for adjusting the seepage face occurring in the downstream boundary of the dams.

We have conducted a series of numerical experiments using our own program, demonstrating the convergence of the loops. In this study, we use an example of a square homogenous embankment dam with the difference in the upstream and downstream water levels, leading to the seepage flow through the dam body. The results show the convergence in the loop for changing the un-saturated hydraulic conductivities and the seepage face. Besides, we have compared our program's results to the ones with the software SEEP/W. The insignificant differences reveal the encouragement of our own program for determining the free surfaces of the seepage mechanism through the homogenous embankment dams.

As we discussed, this program is just a part of an expected future routine used for considering groundwater problems. It is no doubt that our program still has limitations, and some aspects need to be revised such as using higher-degree elements, the meshes that should be finer around the seepage faces, more layers of soils within dam bodies should be used.

Acknowledgement

We acknowledge Ho Chi Minh City University of Technology (HCMUT), VNU-HCM for supporting this study.

References

[1]. S. P. Neuman and P. A. Witherspoon, "Finite Element Method of Analyzing Steady Seepage with a Free Surface," Water Resources Research, vol. 6, no. 3, pp. 889-897, 1970, doi: https://doi.org/10.1029/WR006i003p00889.

[2]. C. S. Desai, "Finite element residual schemes for unconfined flow," International Journal for Numerical Methods in Engineering, vol. 10, no. 6, pp. 1415-1418, 1976, doi: https://doi.org/10.1002/nme.1620100622.

[3]. K.-J. Bathe and M. R. Khoshgoftaar, "Finite element free surface seepage analysis without mesh iteration," International Journal for Numerical and Analytical Methods in Geomechanics, vol. 3, no. 1, pp. 13-22, 1979, doi: https://doi.org/10.1002/nag.1610030103.

[4]. S. J. Lacy and J. H. Prevost, "Flow through porous media: A procedure for locating the free surface," International Journal for Numerical and Analytical Methods in Geomechanics, vol. 11, no. 6, pp. 585-601, 1987, doi: https://doi.org/10.1002/nag.1610110605.

[5]. A. Cividini and G. Gioda, "On the variable mesh finite element analysis of unconfined seepage problems," Géotechnique, vol. 39, no. 2, pp. 251-267, 1989, doi: 10.1680/geot.1989.39.2.251.

[6]. A. Leontiev and W. Huacasi, "Mathematical programming approach for unconfined seepage flow problem," Engineering Analysis with Boundary Elements, vol. 25, no. 1, pp. 49-56, 2001/01/01/ 2001, doi: https://doi.org/10.1016/S0955-7997(00)00067-9.

[7]. J.-P. Bardet and T. Tobita, "A practical method for solving free-surface seepage problems," Computers and Geotechnics, vol. 29, no. 6, pp. 451-475, 2002/09/01/ 2002, doi: https://doi.org/10.1016/S0266-352X(02)00003-4.

[8]. D. G. Fredlund, H. Rahardjo, and M. D. Fredlund, Unsaturated Soil Mechanics in Engineering Practice, 1st ed. Wiley-Interscience, 2012.

[9]. S. P. Neuman, "Saturated-Unsaturated Seepage by Finite Elements," Journal of the Hydraulics Division, vol. 99, no. 12, pp. 2233-2250, 1973, doi: doi:10.1061/JYCEAJ.0003829.

[10]. C. S. Desai and G. C. Li, "A residual flow procedure and application for free surface flow in porous media," Advances in Water Resources, vol. 6, no. 1, pp. 27-35, 1983/03/01/ 1983, doi: https://doi.org/10.1016/0309-1708(83)90076-3.

[11]. A. T. Papagianakis and D. G. Fredlund, "A steady state model for flow in saturated–unsaturated soils," Canadian Geotechnical Journal, vol. 21, no. 3, pp. 419-430, 1984, doi: 10.1139/t84-046.

[12]. D. V. Hutton, Fundamentals of finite element analysis, 1 ed. Boston: McGraw-Hill, 2004.

[13]. M. T. van Genuchten, "A Closed-form Equation for Predicting the Hydraulic Conductivity of Unsaturated Soils," Soil Science Society of America Journal, vol. 44, no. 5, pp. 892-898, 1980, doi: https://doi.org/10.2136/sssaj1980.03615995004400050002x.

[14]. G.-S. I. Ltd., Seepage modelling with SEEP/W. Calgary, Canada: Geo-Slope International Ltd., 2012.

[15]. C. Geuzaine and J.-F. Remacle. "GMSH." https://gmsh.info/ (accessed.